Tracking using Flocks of Features, with Application to Assisted Handwashing

Jesse Hoey
Division of Applied Computing,
University of Dundee,
Dundee DD1 4HN Scotland
jessehoey@computing.dundee.ac.uk

Abstract

This paper describes a method for tracking in the presence of distractors, changes in shape, and occlusions. An object is modeled as a *flock* of features describing its approximate shape. The flock's dynamics keep it spatially localised and moving in concert, but also well distributed across the object being tracked. A recursive Bayesian estimation of the density of the object is approximated with a set of samples. The method is demonstrated on two simple examples, and is applied to an assistive system that tracks the hands and the towel during a handwashing task.

1 Introduction

Tracking an object in the presence of occlusions and distractions is a pervasive problem for computer vision applications. Objects to be tracked usually have some consistent features, are spatially compact, and move cohesively. Typical tracking methods use some model of the appearance of an object to be tracked, and estimate the fit of the model to the object over time. However, in many applications, the object's shape and appearance may change over the course of a sequence. For example, human hands need to be tracked for many human-computer interaction tasks, but change shape and velocity fairly quickly, differences which must be accounted for. The method we present uses a generic type of model: a *flock* of features [9]. The features are characteristics of the local appearance of the object to be tracked, and they are loosely grouped using flocking constraints.

A flock consists of a group of distinct members that are similar in appearance to each other and that move congruously, but that can exhibit small individual differences. A flock has the properties that no member is too close to another member, and that no member is too far from the center of the flock. The flocking concept helps to enforce spatial coherence of features across an object, while having enough flexibility to adapt quickly to large shape changes and occlusions. The concept of a flock comes from natural observation of flocks of birds, schools of fish, or herds of mammals, in which the members must stay close to avoid predators, but must avoid collisions. Flocking concepts have been applied in computer graphics for simulation [12, 13], and in deterministically tracking an object with a moving camera using KLT features [9]. The primary contribution of this paper is the description of an approximate Bayesian sequential tracking method that uses flocks of features to implement spatial, feature and velocity cohesiveness constraints.

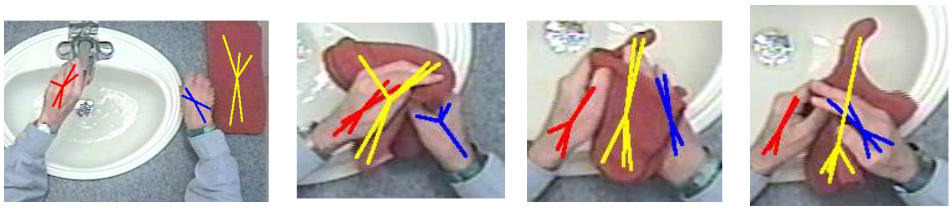

(a) 4974 (b) 5096 (c) 5502 (d) 5576

Figure 1: (a) Three flocks of 5 color features, or *specks*, tracking three objects: two hands and a towel. (b)–(d) during occlusion and shape changes.

This method is robust to partial occlusions, distractors, and shape changes, and is able to consistently track objects over long sequences. The flock does not assume any particular shape, instead adapting the distribution of its members to the current object distribution, which may even be non-contiguous (e.g. in the case of partial occlusions).

Figure 1(a) shows an example of three flocks of 5 color features each tracking two hands and a towel. At the start, the members of each flock are distributed across the objects they are tracking. Figure 1(b)–(d) show the same three flocks tracking the same three objects later in the sequence, during occlusions and shape changes. The flocks are able to maintain a track on the objects, even though their shapes and sizes have changed.

We use an approximate Bayesian sequential estimation technique to track the full posterior distribution over object locations and features. We demonstrate the capabilities of this tracker on a synthetic sequence, and on a real sequence with significant occlusion. We then apply our tracker to an assistive technology scenario, in which a system assists a person with dementia during hand-washing. The system observes the user with a camera mounted above the sink, and tracks the hands and the towel. To allow for very long-term tracking of multiple objects in this case, we use a combination of three mixed-state particle filters [6], with data-driven proposals [11] and simple interactions to enable re-initialisation after a track is lost. A previous system for handwashing [2] used a simple color based location method [10], with no tracking.

There has been much work in the last decade on gesture recognition, typically from the perspective of human-machine interfaces or human-robot interfaces. Most approaches use color and/or motion features, and attempt to recognise predefined motions [4] or hand poses [3]. However, they do not deal well with occlusions or arbitrary shape changes. Recent work deals with occlusions and appearance changes by explicitly building models of image layers and adapting them over time [7], but is too computationally intensive for human interactive systems. Much work on tracking for gesture recognition is focused on dealing with cluttered and changing backgrounds [3, 9], which becomes important when using a moving camera. Our work generalises [9] by tracking the distribution over flocks, but we use a static camera and a fixed background.

2 Flocks of Features

A flock is a loose collection of features, or members. The flock maintains a consistent motion, even though the members are moving independently. This decentralised organisation can be implemented by constraining each member to stay far enough from each other member, yet close enough to the center of the flock [12, 13].

More formally, a flock, $\boldsymbol{\phi}$, is a tuple $\{N_f, \mathbf{W}, \mathbf{v}, \boldsymbol{\theta}_f, \boldsymbol{\xi}_c, \boldsymbol{\xi}_u\}$ where N_f is the number of features in the flock, $\mathbf{W}$ is a set of N_f features, $\mathbf{w}_i = \{\mathbf{x}_i, \boldsymbol{\omega}_i\}_{i=1}^{N_f}$, with image positions $\mathbf{x}_i = \{x_i, y_i\}$, and (as yet unspecified) feature parameters $\boldsymbol{\omega}_i$ that describe how the image should appear given that a feature is present at $\mathbf{x}_i$. The flock has a mean velocity $\mathbf{v} = \{v_x, v_y\}$, and all features in the flock move with the same mean velocity, but with independent (but equal) Gaussian noise, $n_v \sim \mathcal{N}(\mathbf{0}, \boldsymbol{\Sigma}_v)$. The flock also has some model of the mean distribution of its members, $\boldsymbol{\theta}_f$. In the case of simple color features, this model consists of a Gaussian distribution in color space, $\boldsymbol{\theta}_f = \{\mathbf{c}_f, \boldsymbol{\Sigma}_f\}$. Finally, the flock has a set of *collision* parameters $\boldsymbol{\xi}_c$, and a set of *union* parameters, $\boldsymbol{\xi}_u$. The collision parameters are used to define a function of the distance between members of the flock that indicates when a collision is likely to occur. An example is a threshold function, in which case $\boldsymbol{\xi}_c$ is a threshold on the distance. The union parameters, $\boldsymbol{\xi}_u$, are similar, except they define when a member is straying from the flock center. We will see more concrete examples of these parameters and functions in the next section.

The likelihood of observing an image $\mathbf{z}$ given a flock $\boldsymbol{\phi}$, can be computed by assuming that each feature generates parts of the image independently, such that $L(\mathbf{z}|\boldsymbol{\phi}) = \prod_{i=1}^{N_f} L(\mathbf{z}|\mathbf{w}_i, \boldsymbol{\theta}_f)$. In this paper, we will use a simple type of feature, a color *speck*, which is simply a set of $N_p = 4$ pixels in a 2×2 square. Each speck has a *local* Gaussian color model, $\boldsymbol{\theta}_o = \{\boldsymbol{c}_o, \boldsymbol{\Sigma}_o\}$. While this type of simple feature is expressive enough here, other applications may require additional texture or color features. The specks must conform to their flock's color model, $\boldsymbol{\theta}_f$, as well as attempt to each model their local color distribution through $\boldsymbol{\theta}_o$. Finally, a constant "background" density, c_p, is also used for better performance under occlusions. We use the larger of the data likelihood and c_p, thereby allowing some members of the flock to be "lost" (e.g. on an occluding object) without drastically reducing the likelihood of the image given the flock. We can therefore compute the likelihood of an image, $\mathbf{z}$, given a speck, $\mathbf{w}$, in a flock with color model $\boldsymbol{\theta}_f$, as a product over the speck pixels of two Gaussians

$$L(\mathbf{z}|\mathbf{w}, \boldsymbol{\theta}_f) \propto \prod_{j=1}^{N_p} e^{-\gamma_o \min(c_p, \frac{1}{2}(\mathbf{z}_j - \mathbf{c}_o)' \boldsymbol{\Sigma}_c (\mathbf{z}_j - \mathbf{c}_o))} e^{-\gamma_c \min(c_p, \frac{1}{2}(\mathbf{z}_j - \mathbf{c}_f)' \boldsymbol{\Sigma}_f (\mathbf{z}_j - \mathbf{c}_f))} \quad (1)$$

where γ_o and γ_c are parameters that control the tradeoff between the specks obeying their local color models versus adherence to the flock's color model.

3 Sequential Estimation of Flock Density

This section describes how we can estimate the flock density over time using a sequential Markovian process. Let $\boldsymbol{\phi}_t$ denote the flock at time t, and $\mathbf{z}^t = \{z_1 \ldots z_t\}$ be the observations (images) up to time t. Tracking is the estimation of the filtering distribution

$p(\boldsymbol{\phi}_t|\mathbf{z}^t)$. This distribution is updated sequentially using the standard two-step recursion [5], in which $p(\boldsymbol{\phi}_t|\mathbf{z}^t)$ is updated given $p(\boldsymbol{\phi}_{t-1}|\mathbf{z}^{t-1})$ and a new measurement $\mathbf{z}_t$.

$$\textbf{predict}: \qquad p(\boldsymbol{\phi}_t|\mathbf{z}^{t-1}) = \int D(\boldsymbol{\phi}_t|\boldsymbol{\phi}_{t-1})p(\boldsymbol{\phi}_{t-1}|\mathbf{z}^{t-1}) \tag{2}$$

$$\textbf{update}: \qquad p(\boldsymbol{\phi}_t|\mathbf{z}^t) \propto L(\mathbf{z}_t|\boldsymbol{\phi}_t)p(\boldsymbol{\phi}_t|\mathbf{z}^{t-1}) \tag{3}$$

where $L(\mathbf{z}_t|\boldsymbol{\phi}_t)$ is given by Equation 1, and $D(\boldsymbol{\phi}_t|\boldsymbol{\phi}_{t-1})$ is the transition dynamics of a flock. There are three terms in the dynamics,

$$D(\boldsymbol{\phi}_t|\boldsymbol{\phi}_{t-1}) = D'_s(\boldsymbol{\phi}_t|\boldsymbol{\phi}_{t-1})\psi_u(\boldsymbol{\phi}_t)\psi_c(\boldsymbol{\phi}_t), \tag{4}$$

each of which describe a flocking behavior. First, due to the dynamics, D'_s, each feature moves according to the mean velocity of the flock, $\mathbf{v}$, but with added Gaussian noise:

$$D'_s(\boldsymbol{\phi}_t|\boldsymbol{\phi}_{t-1}) = e^{-\gamma_d \sum_{i=1}^{N_f}(\Delta\mathbf{x})'\boldsymbol{\Sigma}_v^{-1}(\Delta\mathbf{x})} \tag{5}$$

where N_f is the number of specks in the flock, $\Delta\mathbf{x} = (\mathbf{x}_{t,i} - \mathbf{x}_{t-1,i} - \mathbf{v}_{t-1})$, $\mathbf{v}_{t-1}$ is the mean velocity of the flock and $\boldsymbol{\Sigma}_v$ is the covariance of the noise in the dynamics, assumed constant for all flock members. The second term in (4) is a penalty for being too close to another flock member, and is implemented using pairwise potentials between members of the flock, expressed as a Gibbs distribution

$$\psi_c(\boldsymbol{\phi}_t) = e^{-\gamma_c \sum_{i=1}^{N_f}\sum_{j=1}^{N_f}\delta(i\neq j)g_c(\mathbf{x}_{t,i},\mathbf{x}_{t,j},\boldsymbol{\xi}_c)},$$

where $g_c(\mathbf{x}_{t,i},\mathbf{x}_{t,j},\boldsymbol{\xi}_c)$ is a penalty function that varies inversely with the distance between $\mathbf{x}_{t,i}$ and $\mathbf{x}_{t,j}$, with parameter $\boldsymbol{\xi}_c$. A similar type of penalty function was also used in [8] to model interaction penalties between different particles in a multi-target tracking example. Here, we apply the same ideas to model interactions between members of the same particle. An example is a simple threshold penalty function, $g_c(\mathbf{x}_{t,i},\mathbf{x}_{t,j},\boldsymbol{\xi}_c) \propto \sigma(|\mathbf{x}_{t,i} - \mathbf{x}_{t,j}|,\boldsymbol{\xi}_c)$, where σ is a sigmoid function, such as

$$\sigma(d,\xi_c) = \frac{1}{1+e^{-a(d-\xi_c)}},$$

where $a < 0$ is a fixed parameter that governs smoothness around the threshold value ξ_c.

The third term in (4) is a penalty for being too far from the center of the flock, also implemented using a potential over the feature locations and the flock mean:

$$\psi_u(\boldsymbol{\phi}_t) = e^{-\gamma_u \sum_{i=1}^{N_f} g_u(\mathbf{x}_{t,i},\overline{\mathbf{x}}_\mathbf{t},\xi_u)},$$

where $\overline{\mathbf{x}}_t$ is the mean position of the flock, and $g_u(\mathbf{x},\overline{\mathbf{x}},\xi_u)$ is a penalty function that is proportional to the distance between $\mathbf{x}$ and $\overline{\mathbf{x}}$, and can be implemented using the same sigmoid as in the collision penalty function, except with $a > 0$.

3.1 Particle Approximation

The general recursions introduced in the previous section yield closed-form expressions only in a limited number of cases, such as when dynamics and likelihood functions are linear Gaussian, resulting in a Kalman filter. In the general case, we wish to deal with functions that may be non-linear and/or non-Gaussian, and so adopt a sequential Monte-Carlo approximation method, also known as a particle filter [5], in which the target distribution is represented using a weighted set of samples.

Let $\mathcal{P}_t = \{N_p, \Phi_t, \mathcal{W}_t\}$ be the particle representation of the target density at time t, where N_p is the number of particles, $\Phi_t = \{\boldsymbol{\phi}_t^{(i)}\}_{i=1}^{N_p}$ are the particles (each is a flock), and $\mathcal{M}_t = \{m_t^{(i)}\}_{i=1}^{N_p}$ are the particle weights with unit sum, $\sum_{i=1}^{N_p} m_t^{(i)} = 1$. The particle filter $\mathcal{P}_t$ approximates the filtering distribution as

$$\overline{p}(\boldsymbol{\phi}_t|\mathbf{z}^t) = \sum_{i=1}^{N_p} m_t^{(i)} \delta_{\boldsymbol{\phi}_t^{(i)}}(\boldsymbol{\phi}_t)$$

where $\delta_{\boldsymbol{\phi}_t^{(i)}}(\boldsymbol{\phi}_t)$ is a Dirac delta function over the space of flocks, with mass at $\boldsymbol{\phi}_t^{(i)}$. Given a particle approximation of $p(\boldsymbol{\phi}_{t-1}|\mathbf{z}^{t-1})$ at time $t-1$, $\mathcal{P}_{t-1}$, and a new measurement (image) at time t, $\mathbf{z}^t$, we wish to compute a new particle set, $\mathcal{P}_t$ that is a sample set from $p(\boldsymbol{\phi}_t|\mathbf{z}^t)$. To do so, we draw samples from a proposal distribution $\boldsymbol{\phi}_t^{(i)} \sim q(\boldsymbol{\phi}_t|\boldsymbol{\phi}_{t-1}^{(i)}, \mathbf{z}_t)$, and compute new (unnormalised) particle weights using [5]:

$$m_t^{(i)} = \frac{m_{t-1}^{(i)} L(\mathbf{z}_t|\boldsymbol{\phi}_t^{(i)}) D(\boldsymbol{\phi}_t^{(i)}|\boldsymbol{\phi}_{t-1}^{(i)})}{q(\boldsymbol{\phi}_t^{(i)}|\boldsymbol{\phi}_{t-1}^{(i)}, \mathbf{z}_t)} \tag{6}$$

The weights are then normalised and possibly resampled if they are too degenerate [1].

3.2 Data-Driven proposal

In cases such as the assistive technology scenario we present in Section 4.3, the tracking must be robust over long periods of time, and must be able to re-initialise if the track is lost, such as when hands leave the scene temporarily. To accomplish this, we augment our tracking method with a mixed state dynamics [6], and a data-driven proposal [11]. A mixed-state tracker has dynamics noise, $\mathbf{\Sigma}_v$, in (5), that varies depending on the *strength* of the particle filter, or how accurately the particle filter is estimated to be tracking. This strength is estimated by comparing the sum of the unnormalised particle weights to a fixed minimum weight, and taking the ratio to a fixed maximum interval. The resulting strength estimate in $[0, 1]$ is then used to set the dynamics noise between fixed bounds.

A data-driven proposal uses samples generated from a combination of the dynamics process and a separate, data-driven process. This idea was used successfully in [11], where an Adaboost process generated particles for the proposal distribution of a mixture of particle filters. To implement these ideas, our proposal distribution includes the expected mean flock dynamics $D'_s(\boldsymbol{\phi}_t|\boldsymbol{\phi}_{t-1}^{(i)})$ (Equation 5), and a second process, $q_d(\boldsymbol{\phi}_t|\boldsymbol{\phi}_{t-1}^{(i)}, \mathbf{z}_t)$, that generates new samples $\boldsymbol{\phi}_t$ directly from a new image $\mathbf{z}_t$. The complete proposal combines these two distributions with a weight α [11]:

$$q(\boldsymbol{\phi}_t|\boldsymbol{\phi}_{t-1}^{(i)}, \mathbf{z}_t) = \alpha q_d(\boldsymbol{\phi}_t|\mathbf{z}_t^j) + (1-\alpha) D'_s(\boldsymbol{\phi}_t^{(i)}|\boldsymbol{\phi}_{t-1}^{(i)}) \tag{7}$$

Data samples are drawn as described below, and weighted using:

$$m_t^{(i)} = \frac{m^* L(\mathbf{z}_t|\boldsymbol{\phi}_t^{(i)}) D_0(\boldsymbol{\phi}_t^{(i)})}{q_d(\boldsymbol{\phi}_t^{(i)}|\boldsymbol{\phi}_{t-1}^{(i)}, \mathbf{z}_t)}, \tag{8}$$

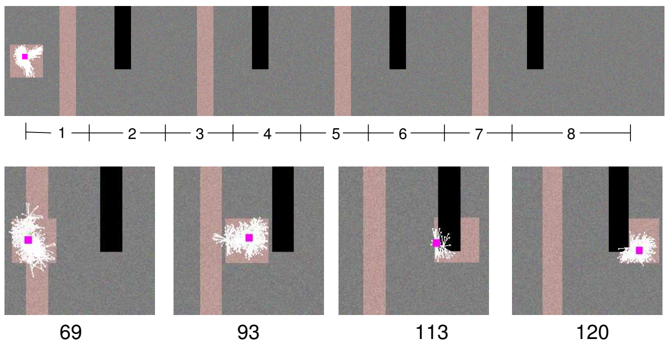

Figure 2: Level 5 simulated sequence, showing (top) the entire image and flocks tracking object, (bottom) close-ups of four key frames showing the flocks dealing with a distractor (frame 69-93) and an occluder (frame 113-120).

where $m^* = (\alpha N_p)^{-1}$ are the prior weights which assume all of the expected αN_p particles will be drawn equally, and $D_0(\boldsymbol{\phi}_t^{(i)}) = D_0'(\boldsymbol{\phi}_t^{(i)})\psi_u(\boldsymbol{\phi}_t)\psi_c(\boldsymbol{\phi}_t)$ includes the collision and union penalty functions, and a prior distribution, $D_0' = N_d^{-N_f}$ is the probability of drawing N_f features independently at random from a set of N_d possibilities, where N_d is the number of valid pixels used in the data proposal.

Our data-driven proposal, q_d, is built by using the model $\boldsymbol{\theta}_f$ for the features of the tracked object to build a probability map over the input image. The probability map is built by thresholding the image in feature space, and median filtering the result to remove small components. We then choose the connected component closest to the particle being updated in this binary image and build a normalised map $P_o(\mathbf{z}_i|\boldsymbol{\theta}) = kPr(\mathbf{z}_i|\boldsymbol{\theta})$ where k is the normalising constant summed over the component being used. Finally, we draw a flock sample from the joint distribution over the N_f feature locations, $Pr(\mathbf{x}_{i=1}^{N_f}|\mathbf{z},\boldsymbol{\theta})$, by sampling each feature independently from P_o,

Once a new set of samples has been drawn, we set the value of α to weight the data-driven proposal in (7) by looking at the filter's current strength, and whether a connected component was found that corresponds to that filter. If no component was found, then $\alpha = 0$, since there will be nothing to draw samples from anyways. Otherwise, we set α closer to 0 the higher the strength. If $s > 0.8$, then we set $\alpha = 0$.

4 Results

In this section, we used the following parameter values, set empirically by hand, unless otherwise specified. The sigmoid parameter is $a = 0.01$. The color density background was $c_p = -\log(10^{-20})$. The weights for dynamics, collision and union terms were $\gamma_d = 1$,$\gamma_c = 20$ and $\gamma_u = 60$, respectively.

4.1 Synthetic Sequences

We compare our tracker against a simple color-based particle filter, where each particle is a *speck* of color (a flock tracker with $N_f = 1$). We ran both trackers with $10, 100$ and 500

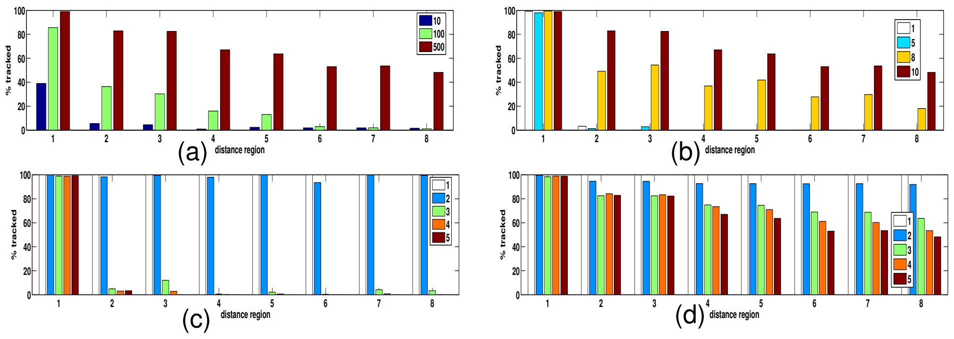

Figure 3: Synthetic results plot the percentage of trials in which the track holds at each region 1-8 (see Figure 2a). A perfect tracker would score 100% at all regions. (a) Level 5 (hardest) problem with flock size $N_f = 10$ for different numbers of particles (10,100,500). (b) Level 5 problem for $N_f = 1, 5, 8, 10$ with 500 particles. (c),(d) $N_f = 1, 10$ trackers, resp., on level 1-5 problems with 500 particles

particles[1]. We used $N_f = 5, 8, 10$ with collision thresholds $\xi_c = 40, 30, 20$, respectively. The union threshold was $\xi_u = 20$, and the dynamics noise was $\Sigma_v = 5.0$ pixels for all trackers.

We evaluate the trackers by running them each 100 times with different initial random seeds and random initializations. At each of the 400 time steps it takes for the square to cross the image from left to right, we count the trials for which the tracker mean is in the square. We then take the mean of these counts over the regions $i \in 1 \ldots 8$ between each distractor or occluder, as shown in Figure 2. Thus, the numbers for each of the 8 regions show how many (out of 100 trials) are still tracking the object at that point. Figure 3(a) shows the behavior of the $N_f = 10$ flock tracker for different numbers of particles $N_p = 10, 100, 500$ for the hardest (level 5) problem. We see that the performance for $N_p = 10$ is poor, but for $N_p = 500$, the tracker tracks half the sequences to the end. Figure 3(b) compares different flock sizes ($N_f = 1, 5, 8$ and 10), again for the hardest problem instance. Here we see the $N_f = 1, 5$ trackers rapidly get lost after the first distractor. The $N_f = 8$ tracker does a little better, tracking fully about 20% of the sequences. The $N_f = 10$ tracker is better able to handle the occlusions because of the reduced collision threshold (ξ_c), allowing it more flexibility.

Figure 3(c) and (d) show the $N_f = 1, 10$ trackers, respectively, for the different difficulty levels (1-5). We see that the $N_f = 1$ tracker is only able to deal with the easiest problems, whereas the $N_f = 10$ still maintains performance for the other difficulty levels.

4.2 Real Sequence

Figure 4(top) shows 4 frames from a 15-frame sequence of a child running behind a black fence and a bush. We used $N_f = 8$, $\xi_c = 20$ and $N_p = 100$. The flocks are able to track the child's jacket, even after shape changes (e.g. the arm extends). The bottom row

[1]Additionally, we ran the simple speck tracker with 5000 particles, since the flock-based tracker with 500 flocks contains 5000 specks in total, but found no significant improvement over 500 particles.

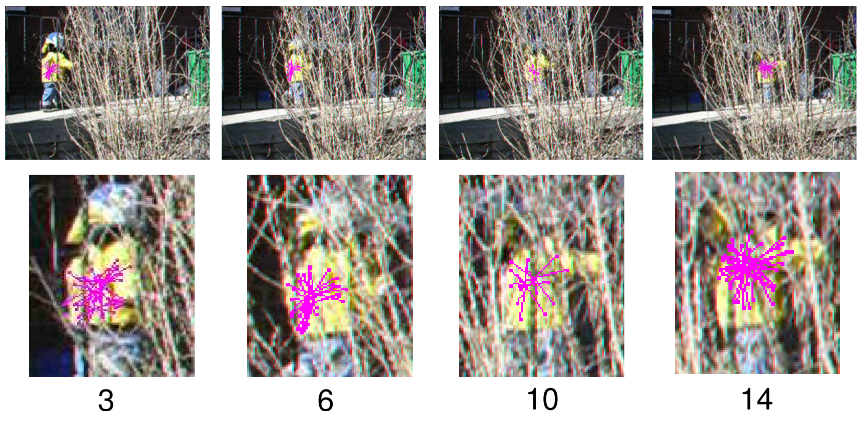

Figure 4: Sequence with occlusion

shows close-ups, with flocks distributed across the jacket, some members on the arm area. In order to evaluate the strength of the threshold c_p, we computed the fraction of specks that had likelihoods below $c_p = -log(10^{-20})$ over the course of this sequence. This fraction was about 17% for the frames in which the child was partially occluded by the bush, indicating that, although the background density is useful, it is not dominant.

4.3 Handwashing Tracking

The goal in the handwashing task is to monitor a person's progress, and to issue verbal or visual prompts when the person needs assistance [2]. A fundamental building block in such a system is the ability to locate and track the person's hands in the sink area. We wish to know, for example, if they are using the soap, the taps, if they are under the water, or if they are in contact with the towel. In our data, the only objects that are not fixed in space are the hands and the towel. Thus, we use three independent particle filters, one for each of the right and left hands, and one for the towel. We use independent particle filters in this paper for simplicity, but our methods could apply to a mixture of particle filters [14], or another type of multiple-target tracking Monte-Carlo method [8].

We used sequences taken from a clinical trial in which an automated prompting system monitored prompted persons with moderate to severe Alzheimer's disease. The video was taken from an overhead SONY CCD DC393 color video camera at $30fps$, and a 570×290 pixel region around the sink was cropped. We used 200 particles and could perform updates of all three filters at over 13 frames per second. We evaluated the tracker by looking at whether the mean flock position was inside the hands or towel region in each frame for 1300 frames from a single user's sequence during which the the user was drying their hands. We compare our method to a simple heuristic that looks only at the connected components from the thresholded images (using $\boldsymbol{\theta}_f$). We find our method makes no errors (0%) in locating the towel during the extreme occlusions compared to 7.4% for the heuristic method. The error rates for hand locations were 2.4% for our method vs. 5.3% for the heuristic method. The errors for our method in locating the hands were due to one hand's flock migrating close to the other hand when the hands were close. These errors could be reduced by using a more sophisticated multi-object

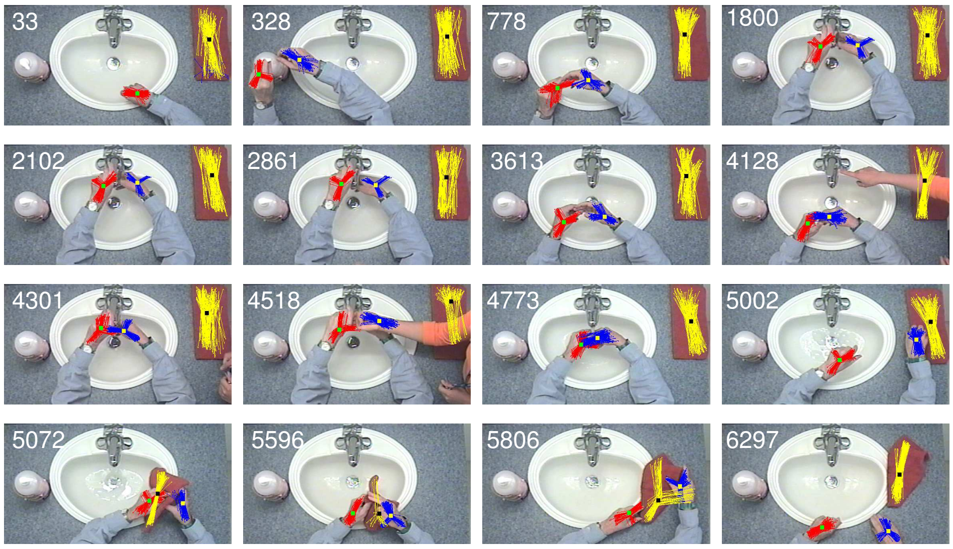

Figure 5: Key frames from full handwashing sequence of 6300 frames (about 4 minutes).

tracking method. We also tested our method on 6 sequences from two different users, and measured the number of tracker failures. We only looked a frames in which both hands were present and a least one was partially visible, and in which the caregiver was not present. A tracker failure was noted either if the hands were separated but one was not tracked, or if both hands were present and together (e.g. when being rubbed together) but neither hand was tracked, or if the towel was not tracked. We found error rates of only 1.9% over a total of 16986 frames in 3 sequences for one user and 0.8% over a total of 7285 frames in 3 sequences for the other. The majority of tracker failures happened after an abrubt change in hand motion, due to our constant velocity assumption. The tracker was consistently able to recover after all tracker failures within about 10 frames.

Figure 5 shows an example of the tracker during a sequence of about 6300 frames. The data-driven proposal was only used for 23 frames of this sequence, primarily during resets when the hands were close. At the top left (frame 33), the right hand and the towel are being tracked, while the left hand particle filter cannot gain strength. The left hand filter uses $\alpha = 0$, however, since there is no component available for it to use. The user applies soap and then attempts to turn on the water. At frame 4128, the caregiver steps in, but the trackers remain undistracted until frame 4518, when one of the user's hands is completely occluded, and one tracker starts to track the caregiver's left hand[2]. Some frames of interest are 2102 where the right hand filter has some flock members off the hand completely, and frame 5806, where some members of the towel flocks are on the right hand, but the towel mean is still centered on the towel. The speck likelihoods allow for this flexibility. Close-up examples from this sequence can also be seen in Figure 1.

[2]The tracker would be paused during the caregiver's interaction. Otherwise, additional filters would be required. The tracker automatically resets itself after about a second after the occluding hand leaves the scene.

5 Conclusion

We have introduced a particle filter tracking technique based on flocks of features and have shown how it can be used to track objects under occlusions and distractions, and in an assisted living task. Future work includes using a more sophisticated multi-object tracking model, experimenting with more complex image features, and looking in more depth at the relationships between flock constraints and tracked object shapes.

Acknowledgements: This work was done while the author was at the University of Toronto, and was supported by Intel Corporation and the American Alzheimer Association.

References

[1] Sanjeev Arulampalam, Simon Maskell, Neil Gordon, and Tim Clapp. A tutorial on particle filters for online nonlinear/non-gaussian bayesian tracking. *IEEE Transactions on Signal Processing*, 50(2):174–189, 2002.

[2] Jen Boger, Pascal Poupart, Jesse Hoey, Craig Boutilier, Geoff Fernie, and Alex Mihailidis. A decision-theoretic approach to task assistance for persons with dementia. In *Proc. IEEE International Joint Conference on Artificial Intelligence*, pages 1293–1299, Edinburgh, July 2005.

[3] Lars Bretzner, Ivan Laptev, and Tony Lindeberg. Hand gesture recognition using multi-scale colour features, hierarchical models and particle filtering. In *Proceedings of IEEE Intl. Conf. on Face and Gesture Recognition*, pp. 423–428, 2002.

[4] Ross Cutler and Matthew Turk. View-based interpretation of real-time optical flow for gesture recognition. In *Proc. Intl. Conf. on Automatic Face and Gesture Recognition*, p. 98–104, Nara, Japan, April 1998.

[5] Arnaud Doucet, Nando de Freitas, and Neil Gordon, editors. *Sequential Monte Carlo in Practice*. Springer-Verlag, 2001.

[6] Michael Isard and Andrew Blake. A mixed-state condensation tracker with automatic model-switching. In *Proc 6th Int. Conf. Computer Vision*, 1998.

[7] Allan D. Jepson, David J. Fleet, and Michael J. Black. A layered motion representation with occlusion and compact spatial support. In *Proc. of ECCV 2002*, Copenhagen, Danemark, May 2002.

[8] Zia Khan, Tucker Balch, and Frank Dellaert. MCMC-based particle filtering for tracking a variable number of interacting targets. *IEEE Transactions on Pattern Analysis and Machine Intelligence*, 27(11):1805–1918, November 2005.

[9] Mathias Kölsch and Matthew Turk. Fast 2d hand tracking with flocks of features and multi-cue integration. In *IEEE Workshop on Real-Time Vision for Human-Computer Interaction*, Washington, DC, 2004.

[10] Alex Mihailidis, Brent Carmichael, and Jen Boger. The use of computer vision in an intelligent environment to support aging-in-place, safety, and independence in the home. *IEEE Transaction on Information Technology in Biomedicine (Special Issue on Pervasive Healthcare)*, 8(3):1–11, 2004.

[11] Kenji Okuma, Ali Taleghani, Nando de Freitas, James J. Little, and David G. Lowe. A boosted particle filter: Multitarget detection and tracking. In Springer-Verlag, editor, *Proceedings of European Conference on Computer Vision (ECCV)*, volume 3021 of *LNCS*, pages 28–39, 2004.

[12] William T. Reeves. Particle systems - a technique for modeling a class of fuzzy objects. *ACM Transactions on Graphics*, 2(2):91–108, April 1983.

[13] Craig W. Reynolds. Flocks, herds, and schools: A distributed behavioral model. In *Computer Graphics*, volume 21 (4), pages 25–34. ACM SIGGRAPH, 1987.

[14] Jaco Vermaak, Arnaud Doucet, and Patrick Pérez. Maintaining multi-modality through mixture tracking. In *Proceedings of Ninth IEEE International Conference on Computer Vision (ICCV)*, Nice, France, October 2003.